Target Z dependence and additivity of cross sections for electron loss by 6-MeV/amu Xe^{18+} projectiles

R. L. Watson, Yong Peng, V. Horvat, and G. J. Kim
Cyclotron Institute and Department of Chemistry, Texas A&M University, College Station, Texas 77843

R. E. Olson
Physics Department, University of Missouri–Rolla, Rolla, Missouri 65401
(Received 21 October 2002; published 14 February 2003)

The dependence of electron loss by 6-MeV/amu Xe^{18+} on target atomic number was investigated by measuring single-collision cross sections for loss of one to eight electrons in targets of the noble gases He, Ne, Ar, Kr, and Xe. The total-electron-loss cross sections were found to increase linearly with target atomic number, but an abrupt slope change was observed to occur between Ne and Kr. Calculated total-loss cross sections obtained using the n-body classical trajectory Monte Carlo method were in good agreement with the measurements. The dependence of the individual cross sections on the number of electrons lost was reasonably well represented by a semiempirical fitting procedure utilizing the independent-electron approximation. Additional measurements performed with a variety of molecular targets provided a rigorous test of cross-section additivity. It was found that the additivity rule works well in this collision regime and that the molecular nature of the target has remarkably little influence on the cross sections.

DOI: 10.1103/PhysRevA.67.022706 PACS number(s): 34.50.Fa

I. INTRODUCTION

The ionization and electron transfer mechanisms that determine the charges of energetic ions passing through matter have been of continuing interest since the discovery of natural radioactivity. The close connection between the charge of an ion and the strength of its Coulomb interaction with atoms of the medium makes it one of the most important factors in determining the rate of energy loss or stopping power. Consequently, new information pertaining to the fundamental atomic collision processes responsible for the evolution of fast-projectile charge-state distributions is of potential interest to many areas of basic and applied research. Recent activity has focused on electron-loss collisions of heavy ions with atomic numbers $\geqslant 54$ because of their potential application in heavy-ion-induced inertial-confinement fusion [1–4].

The main features of single-electron loss in collisions involving relatively light projectiles and targets are reasonably well reproduced by theoretical treatments based on the plane-wave Born approximation [5,6]. However, simple first-order theories are incapable of correctly accounting for the screened electron–target-nucleus interactions and hence they are unreliable when applied to many-electron heavy-ion atom collision systems [7]. Furthermore, cross sections for multielectron loss obtained using the results of single-electron-loss calculations via the independent-electron approximation (IEA) do not take into account the large changes in ionization energy that occur as the outer-shell electrons are successively removed [1] and tend to overestimate the cross sections for multiple ionization [8]. So far, the only method that overcomes this problem and explicitly includes both the electron-electron and the screened nuclear-electron interactions is the n-body classical trajectory Monte Carlo (n-CTMC) method developed by Olson [9]. However, application of this method to the collision regime considered here has been of limited success. For example, predicted cross sections for loss of one through three electrons from (2–9)-MeV/amu Xe^{18+} ions in N_2 were found to be in fair agreement with experiment, but those for the loss of four and five electrons decreased much more rapidly as a function of projectile energy than the experimental cross sections [4].

In view of the present evolutionary state of theory, experimental data are needed to test new theoretical developments and to establish the systematic dependence of charge-changing cross sections for heavy collision systems on the relevant collision parameters, such as projectile atomic number (Z_1), velocity (v_1), and charge (q), and target atomic number (Z_2). The present work was undertaken to examine the dependence of cross sections for single- and multiple-electron loss from 6-MeV/amu Xe^{18+} projectiles on target atomic number. Information of this type for multiple-electron loss from high-Z_1 heavy-ion projectiles is extremely sparse, and, to our knowledge, currently extends only up to $Z_1 = 26$ [10,11]. Cross sections for single- and multiple- (up to eight) electron loss in noble-gas targets of He, Ne, Ar, Kr, and Xe are presented herein.

A second objective of the present measurements was to test the additivity of electron-loss cross sections for molecular targets. It is often assumed that the cross section for a collision process involving the interaction of a fast ion with a molecular target can be approximated by adding up the individual cross sections for the constituent atoms of the molecule. This so-called additivity rule is generally hard to justify on theoretical grounds, but in the absence of experimental cross sections for molecular targets, it is usually the only alternative available. It is well known, for example, that an additivity rule (i.e., the Bragg rule) provides a reasonably accurate account of stopping powers for heavy ions traveling in solid materials composed of chemical compounds [12]. On the other hand, Wittkower and Betz [13]

measured electron-capture and -loss cross sections for 12-MeV I^{5+} ions in a variety of molecular targets and found that the additivity rule overpredicted some cross sections by more than a factor of 2. Based on their results, these authors concluded that a collision between a relatively low-velocity heavy ion and a complex molecular target cannot, in general, be treated as a sequence of successive collisions with the individual atoms of the molecule. Bissinger *et al.* [14] found that cross sections for electron capture by (0.8–1)-MeV protons colliding with hydrocarbon gases are as much as 23% smaller than those predicted by the additivity rule. They attributed this additivity failure to intramolecular electron-loss processes operating on neutral H atoms (i.e., protons that had already captured an electron) during their exit from target molecules. Recently, Sanders *et al.* [15] measured electron-loss cross sections for neutral H atoms colliding with hydrocarbon gases at energies ranging from 60 to 120 keV and found their cross sections to be in agreement with the additivity rule. They argued that ''exit effects'' were unimportant in this case because the electron-loss cross section was much larger than the electron-capture cross section, making it unlikely that a H^+ ion would capture an electron on the way out of the target molecule.

In the present work, the question of cross-section additivity is examined in a higher-projectile-Z and -velocity regime than previously by comparing measured electron-loss cross sections for the molecular targets H_2, CH_4, C_3H_8, SiH_4, N_2, CO, CO_2, O_2, C_3F_8, CF_4, and SF_6 with those predicted using the Z_2 dependence established by the noble-gas measurements.

II. EXPERIMENTAL PROCEDURE AND DATA ANALYSIS

The experimental apparatus and methods employed in the present measurements were essentially the same as those described in Ref. [4]. Therefore, only a brief summary will be presented here. A 6-MeV/amu Xe^{18+} beam was extracted from the Texas A&M superconducting cyclotron and directed through a bending magnet into the target chamber. The bending magnet removed ions that had undergone charge-changing collisions with the background gas on their journey from the cyclotron. The beam next passed through a series of three collimators having diameters 1, 2, and 1 mm in order of sequence, and then on into a windowless, differentially pumped gas cell through a 2-mm aperture. The effective length of the gas cell was 2.08 cm, as estimated using the method suggested by Toburen *et al.* [16,17]. After exiting the gas cell through a 2-mm aperture, the beam passed between the poles of a charge-dispersion magnet into a one-dimensional position-sensitive microchannel plate detector (PSD). This detector had an active length of 10 cm and width of 1.5 cm, and a resistive anode was used to measure particle positions by the standard charge-division method. In order to prevent gain shifts and pileup problems in the processing of the signals from the PSD, the counting rates were kept below 2000 s^{-1}. Monitoring and regulation of the gas pressure was accomplished by means of a Baratron pressure transducer and a motorized flow valve, operating in conjunction with an automatic control unit. The pressure remained constant to within $\pm 0.6\%$ over the $\sim$20 min time period of a typical measurement.

Cross sections were determined using the growth-curve method. Accordingly, charge- (position-)distribution spectra were measured at eight different pressures ranging, in most cases, from zero to 64 mTorr. Exceptions were the light target gases H_2 and He, for which measurements were performed at pressures as high as 200 mTorr. The growth curve for a specified charge state i was obtained by plotting its charge-state fraction F_i versus π, where π is the product of the atom or molecule density and the effective gas cell length. Each charge-state fraction was obtained by dividing the number of counts in the corresponding peak appearing in the position spectrum by the total number of detected ions. Over the range of pressures employed, the growth curves were well represented by second-order polynomials $F_i(\pi) = \alpha + \beta\pi + \gamma\pi^2$. The first term represents the background fraction of ions created in collisions with residual gas in the beamline, the second term represents the fraction of ions created in single collisions with the target gas, and the last term represents the fraction of ions created in double collisions with the target gas. Therefore, the desired single-collision cross section for changing from incident charge q to final charge i was obtained from the best-fit value of the parameter β.

During the course of this study, several checks were performed to ensure that the relative detection efficiency of the PSD remained uniform along the length of the detector. The experimental details are discussed in Ref. [4]. In addition, growth-curve measurements with a Ne target were repeated five times, and growth-curve measurements for Ar, Kr, and Xe were each repeated three times in different cyclotron runs. In all cases, several different detectors were used. The *largest* root mean square deviations of the cross sections ranged from 7.3% for one-electron loss to 8.1% for eight-electron loss. This comparison provided a good basis for the estimation of errors in the cross sections arising from variations in detector response and inaccuracies in peak integrations due to background. Additional errors attributed to inaccuracies in the measurement of the absolute pressure and determination of the gas cell effective length are estimated to be 5% and 2%, respectively.

III. RESULTS AND DISCUSSION

A. Target Z dependence

Electron-loss cross sections obtained in measurements with the noble-gas targets are presented in Table I. In all cases except He, individual cross sections are listed for a charge change (Δq) of 1 to 8. Each entry listed for $\Delta q \geqslant 9$ (Ne through Xe) was determined from a composite growth curve constructed by summing the charge fractions of all statistically significant peaks in the charge distribution above that for $\Delta q = 8$.

The dependence of the total-electron-loss cross section on target atomic number is shown in Fig. 1. It may be seen that the data appear to lie along two straight lines, with the He

TABLE I. Electron-loss cross sections (Mb/atom) and fitting parameters for 6-MeV/amu Xe^{18+} ions in noble-gas targets.

Δq	He	Ne	Ar	Kr	Xe
1	3.0±0.2	16±1	24±2	27±2	34±3
2	1.7±0.2	7.8±0.7	11±1	13±1	16±1
3	0.19±0.03	3.8±0.3	5.6±0.5	7.2±0.7	9.0±0.8
4	0.08±0.01	2.9±0.2	4.1±0.3	5.3±0.4	6.7±0.5
5	0.021±0.005	2.0±0.1	3.2±0.2	4.5±0.3	5.6±0.4
6		1.33±0.09	2.7±0.2	3.8±0.3	4.7±0.4
7		0.85±0.07	2.5±0.2	3.5±0.3	4.6±0.4
8		0.47±0.05	1.8±0.2	3.1±0.3	3.8±0.4
⩾9		0.33±0.04	2.2±0.3	7.3±0.9	12±1
Total	4.9±0.3	36±2	56±2	75±3	95±4
p_0	0.213	0.828	0.975	1.000	1.000
δ (Å)	0.076	0.133	0.167	0.193	0.215

and Ne points defining a line having a relatively steep slope and the rest of the points defining a line having a significantly smaller slope. The equations of these two line segments are

$$\sigma = \begin{cases} 3.821Z_2 - 2.7 & \text{for } Z_2 \leqslant 10, \\ 1.076Z_2 + 36.7 & \text{for } Z_2 \geqslant 18, \end{cases} \quad (1)$$

with σ in units of megabarns. This behavior is remarkably similar to that observed by Alton *et al.* [11] for 0.36-MeV/amu Fe^{4+} ions and by Graham *et al.* [18] for 4.66-MeV/amu Pb^{54+} ions. Alton *et al.* also found that a modified Bohr formula, which predicts a $(Z_1^{1/3}+Z_2^{1/3})^2$ dependence [19], yielded cross sections in good agreement with their measurements for one-electron loss. However, application of this formula to the present collision systems results in one-electron-loss cross sections that are too small by a factor ranging from 1.7 for He to 8.5 for Xe.

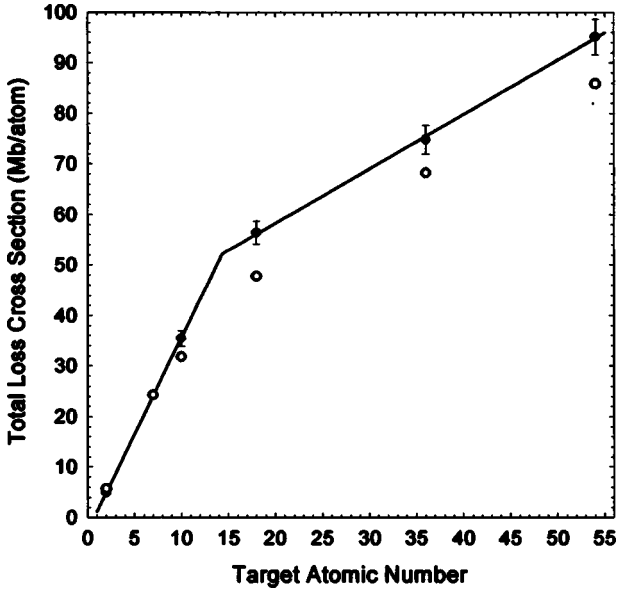

FIG. 1. Total-electron-loss cross sections for 6-MeV/amu Xe^{18+} projectiles in noble-gas targets. Experimental values are shown by filled circles and the results of *n*-CTMC calculations are shown by unfilled circles. The solid lines have been fitted to the experimental data.

The results of *n*-CTMC calculations also are shown in Fig. 1. For these calculations, 18 electrons were centered on the Xe ion in order to model the $3d^{10}4s^24p^6$ electrons. The overall agreement with experiment is quite good and the slopes of the two straight-line segments are accurately predicted. The *n*-CTMC model is really an independent-event model rather than an independent-particle model because the bound electrons are assigned their actual ionization energies, which increase sequentially as electrons are removed. Inclusion of multiple excitation of the electrons, leading to further ionization, is accounted for via an energy deposition model which helps in the description of the high stages of ionization [4].

Since the above results were in reasonable accord with the data, further calculations were performed for unscreened targets (i.e., for bare-ion Coulombic charge centers). The object of this investigation was to deduce the effective atomic number (Z_{eff}) of each noble-gas target by finding the atomic number of the bare ion that yielded the same calculated total-electron-loss cross section as that measured for the noble gas. The results are shown in Fig. 2. The values of Z_{eff} obtained by normalizing the measured cross sections to the smooth curve established by the calculated points are 1.6, 7.5, 10.8, 13.8, and 17.0 for He, Ne, Ar, Kr, and Xe, respectively. It was concluded, therefore, that the He and Ne experience only limited nuclear screening from the *K*-shell electrons, while the nuclear charges of the heavier noble-gas targets are more highly screened by the *L* and higher shells. The change from *K*-shell to longer-range screening of the target nucleus appears to be responsible for the change in the slope of the Z dependence exhibited by the data in Fig. 1.

It is also of interest to note that the calculated Xe^{18+} total-electron-loss cross section is approximately linear in the unscreened nuclear charge, as shown in Fig. 2. One would have expected a Z^2 dependence as predicted by the Born or

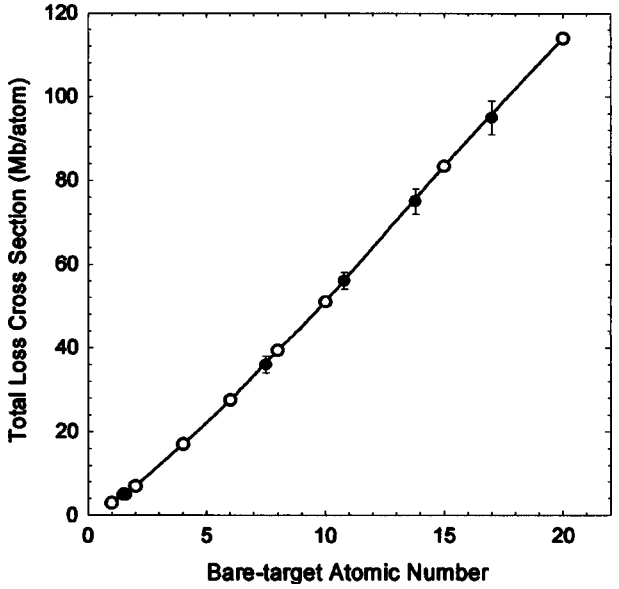

FIG. 2. Calculated (*n*-CTMC) total-electron-loss cross sections for bare targets (unfilled circles) and measured cross sections plotted at the effective atomic numbers required to coincide with the bare-target results (filled circles).

binary encounter approximations. However, these theories are based on a single electron which is not the case at hand. Since the target is completely unscreened, the linear cross-section dependence is due to the electronic structure of the Xe^{18+} projectile. Energy is transferred to projectile electrons whose orbital velocities are comparable to the collision velocity. This yields electron-removal cross sections that are linear in charge state, as has been observed for target ionization by multiply charged projectiles [20]. The basis for such scaling is that the force on the ionized-projectile electron by the two nuclei is comparable during velocity matching conditions.

Cross sections for electron loss as a function of the number of electrons removed from the projectile, $\sigma(\Delta q)$, are shown in Fig. 3. The cross sections for the He target are reasonably well represented by a single exponential function, whereas the cross sections for the other targets display a dependence on Δq that requires two exponential components to describe (similar to a two-component decay curve). This is because the rate of decrease in cross sections for $\Delta q \geqslant 4$ as a function of Δq slows dramatically with increasing target atomic number. Unfortunately, the fitting parameters associated with this representation of the data do not display a smooth, systematic variation as a function of Z_2, and hence it does not provide a reliable means for estimating $\sigma(\Delta q)$ at other values of Z_2.

The possibility of using the IEA in conjunction with a simple empirical ionization probability function to develop a semiempirical method for systematizing the $\sigma(\Delta q)$ was explored. Two probability functions were tried: an exponential $p(b)=p_0\exp(-b/r)$, and a Gaussian $p(b)=p_0\exp(-b^2/2\delta^2)$, where b represents the impact parameter relative to the target nucleus and p_0, r, and δ are fitting

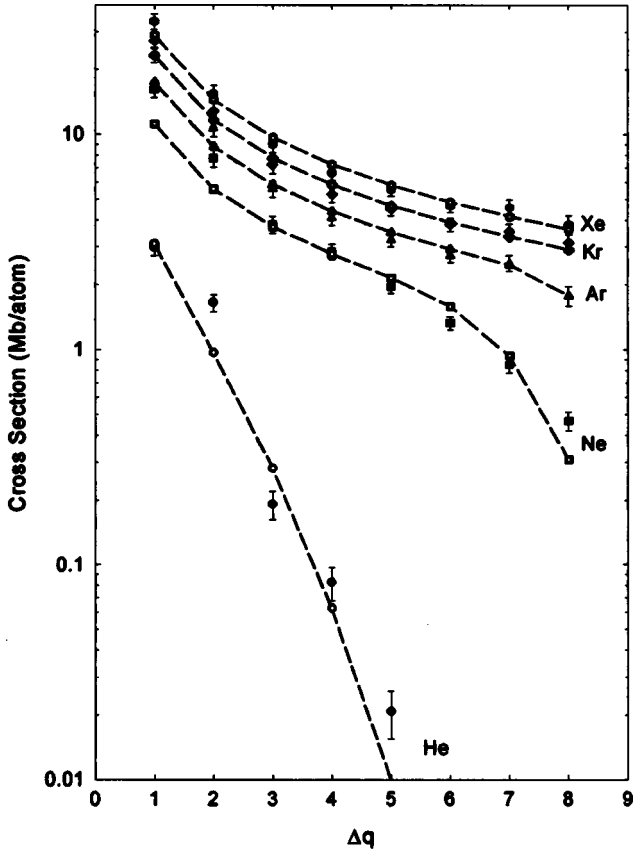

FIG. 3. Electron-loss cross sections plotted as a function of the number of electrons removed from the incident Xe^{18+} projectile (filled symbols). The dashed lines and unfilled symbols show the results of fits to the data using the semiempirical IEA prescription described in the text.

parameters. Detailed descriptions of this procedure, which has often been employed in studies of target-recoil ion production by heavy-ion projectiles, may be found in Refs. [21–24]. In the present application, only the eight outer-shell electrons were considered. The best least-squares fits to the measured $\sigma(\Delta q)$ were obtained with the Gaussian function and are shown by the dashed lines in Fig. 3. The average absolute differences between the fitted and measured cross sections are 34%, 17%, 9%, 8%, and 7%, respectively, for He, Ne, Ar, Kr, and Xe. The resulting values of the two fitting parameters (p_0 and δ) are listed in Table I and they are accurately reproduced by the empirical formulas

$$p_0 = 0.999\exp(-y), \quad \text{where}$$

$$y = \exp[-(Z_2-3.657)/3.802], \tag{2}$$

$$\delta = (1+0.333Z_2)/(19.30+1.296Z_2). \tag{3}$$

B. Molecular targets and cross-section additivity

The total-electron-loss cross sections divided by the number of atoms per molecule (i.e., the total average cross sections per atom) are shown in Fig. 4, plotted as a function of

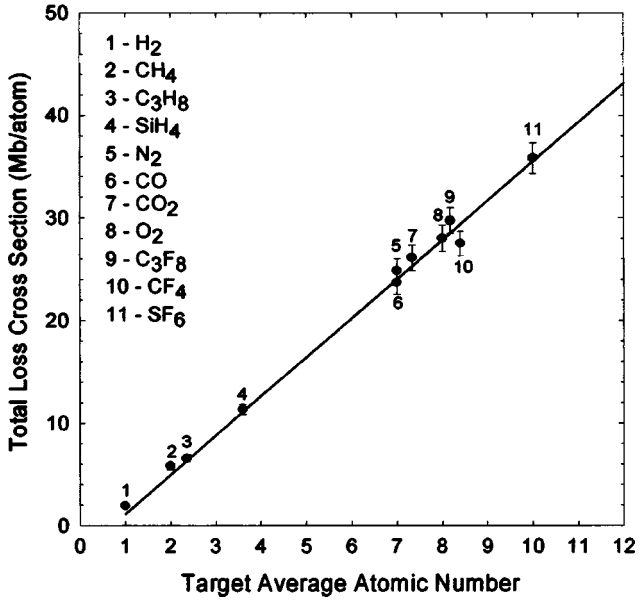

FIG. 4. Total-electron-loss cross section (per atom) for 6-MeV/amu Xe^{18+} projectiles in various molecular targets plotted versus the target average atomic number. The solid line is the same line that was fitted through the He and Ne data points in Fig. 1.

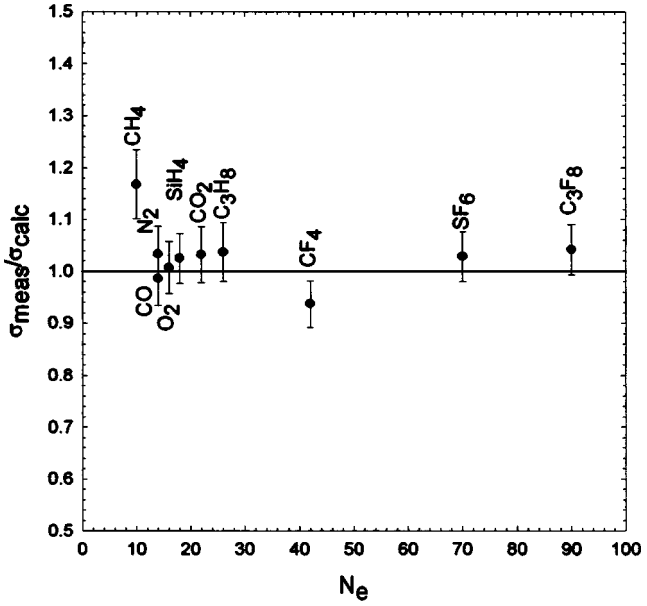

FIG. 5. Ratio of the measured total-electron-loss cross section and that calculated using the additivity rule expressed by Eq. (4), plotted versus the total number of target electrons.

the target average atomic number. The target average atomic number is defined as $\overline{Z}=\Sigma_i f_i Z_i$ where f_i is the fraction of atoms in the molecule having atomic number Z_i. The solid line in Fig. 4 is the same line defined by the total-electron-loss cross sections for the monatomic targets He and Ne in Fig. 1. It is evident that the per atom total-electron-loss cross sections for the molecular targets (a) increase linearly with target average atomic number, and (b) closely correspond to the predicted cross sections for atomic targets having $Z=\overline{Z}$. This latter observation means that the following additivity rule applies to the molecular data:

$$\sigma_{\mathrm{mol}}=N\sigma(\overline{Z}), \tag{4}$$

where σ_{mol} is the cross section per molecule, N is the number of atoms per molecule, and $\sigma(\overline{Z})$ is the cross section for an *atom* having an atomic number equal to the average atomic number of the molecule.

The usual form of the additivity rule is

$$\sigma_{\mathrm{mol}}=\sum_i n_i\sigma(Z_i), \tag{5}$$

where n_i is the number of atoms in the molecule with atomic number Z_i. The validity of this rule was tested by using the linear relationship between the total-loss cross section and the target atomic number, as defined by the noble-gas data [Eq. (1)], to calculate the $\sigma(Z_i)$. The results are shown in Fig. 5, where the ratio of the measured cross section and the cross section calculated using Eq. (5) is plotted versus the total number of electrons per molecule. Except for the H_2 (not shown; ratio $=1.7\pm0.3$) and CH_4 targets, the additivity rule yields total-electron-loss cross sections that are within 6% or less of the measured values. The large ratio exhibited by H_2 may indicate that the Z_2 dependence of the total-electron-loss cross section becomes nonlinear for atomic targets having $Z_2<2$. However, similar large deviations from

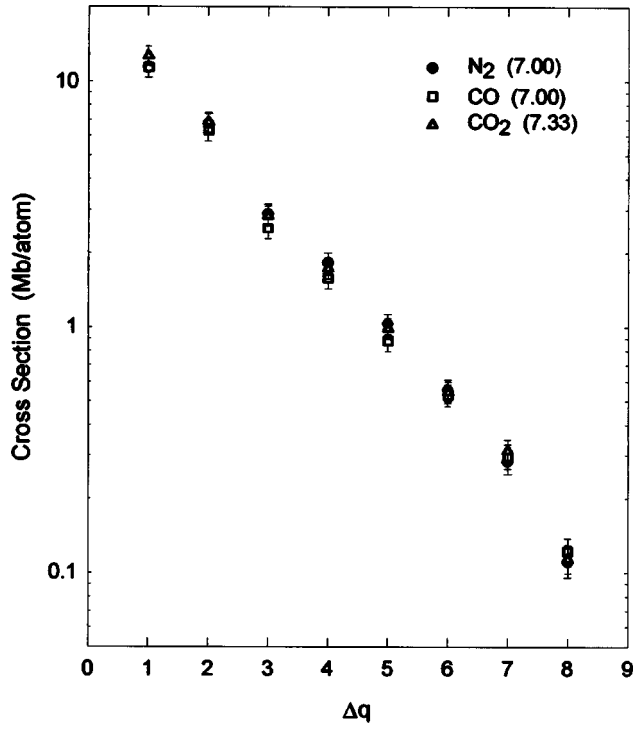

FIG. 6. Comparison of cross sections for the loss of one to eight electrons in the molecular targets N_2, CO, and CO_2. Average atomic numbers are indicated in parentheses.

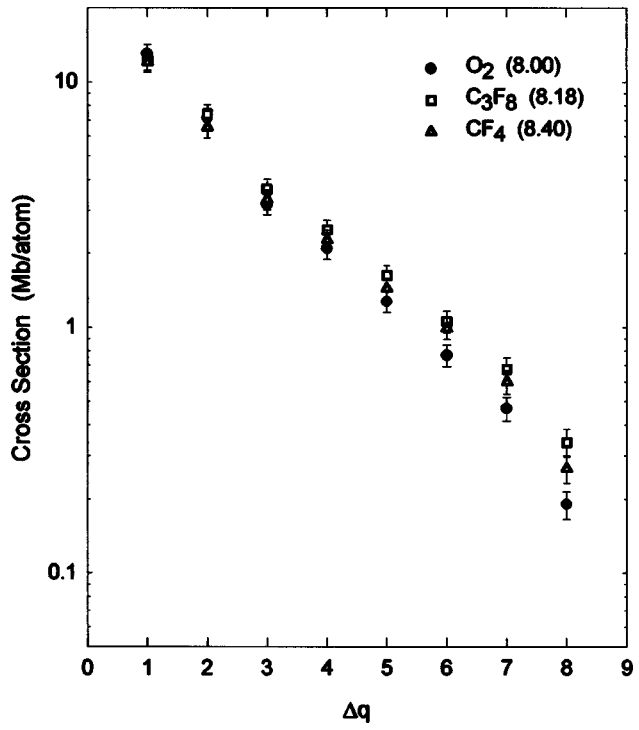

FIG. 7. Comparison of cross sections for the loss of one to eight electrons in the molecular targets O_2, C_3F_8, and CF_4. Average atomic numbers are indicated in parentheses.

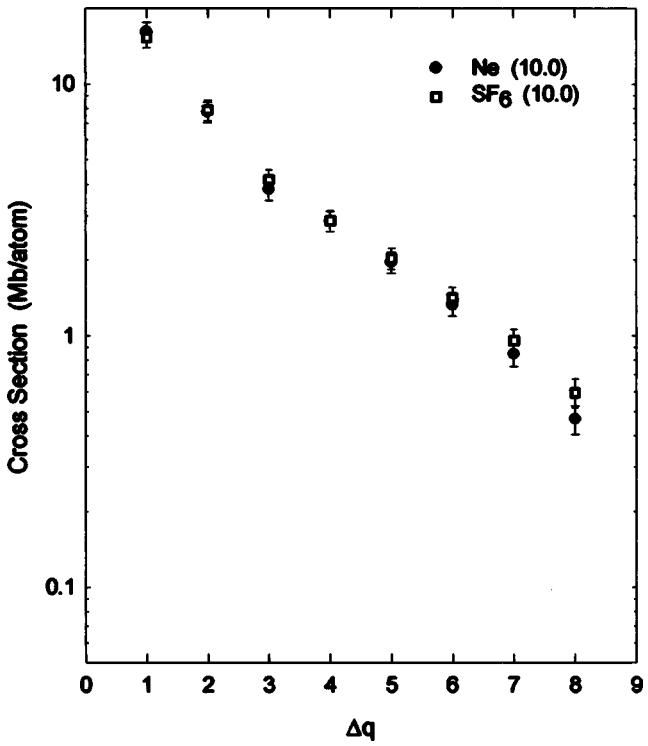

FIG. 8. Comparison of cross sections for the loss of one to eight electrons in the atomic target Ne and the molecular target SF_6. Average atomic numbers are indicated in parentheses.

additivity have been observed in cross sections for single-electron capture by heavy ions from H_2 targets. An analysis based on the Bohr-Lindhard model presented by Knudsen *et al.* [25] predicts a limiting value for the single-electron-capture cross section ratio $\sigma(H_2)/\sigma(H)$ of 3.8 for $E/q^{4/7} > 10^2$, where E is the projectile energy in units of keV/amu. Rather coincidentally, the ratio of the present total-electron-loss cross sections obtained using Eq. (1) to calculate $\sigma(H)$ is 3.4.

In Figs. 6 and 7, the $\sigma(\Delta q)$ are compared for molecular targets having nearly the same average atomic numbers. These figures show that the electron-loss cross sections for specific Δq are remarkably similar for targets within the same $\overline{Z}$ group. However, a slight dependence of the cross sections on the number of atoms per molecule may be indicated by the data in Fig. 7, especially at the higher values of Δq. It would seem reasonable to expect this to be the case, since the more atoms a molecule contains, the more likely it is that the projectile will experience multiple electron-nucleus interactions while traversing the molecule. A comparison of the cross sections for the atomic target Ne and the molecular target SF_6 is shown in Fig. 8. The atomic number of Ne is the same as the average atomic number of SF_6. It appears that the cross sections for high Δq are somewhat larger in the molecular target, but the effect is surprisingly weak.

IV. CONCLUSIONS

Cross sections for the loss of one through eight electrons from 6-MeV/amu Xe^{18+} in single collisions with noble-gas atoms have been measured. The observed dependence of the total-electron-loss cross sections on target atomic number is defined by two straight-line segments, one extending from He to Ne with a relatively steep slope and the other extending from Ar to Xe with a much smaller slope. The predictions of *n*-body CTMC calculations are in good agreement with the total-electron-loss cross sections and reproduce the main features of the observed Z_2 dependence. An investigation of the effect of screening on the electron-loss cross sections suggested that the slope change observed in the Z_2 dependence of the total-electron-loss cross section above $Z_2 = 10$ is associated with the transition from limited screening by K electrons to more effective, longer-range screening by L- and higher-shell electrons.

The individual cross sections for the He target were found to decrease exponentially with increasing numbers of electrons removed, while those for the other noble-gas targets were characterized by a much slower rate of decrease at the higher values of Δq. A semiempirical fitting procedure employing the IEA provided a reasonably good representation of the cross sections for all of the noble-gas targets.

The total-electron-loss cross sections measured with a variety of molecular targets, when divided by the number of atoms per molecule and plotted versus target average atomic number, closely mirrored the straight-line Z_2 dependence established by the cross sections for the atomic targets He and Ne. It was concluded that cross-section additivity works well for electron loss from heavy ions in the present energy and charge regime. This implies that the target molecules act as

assemblies of individual atoms and that alterations of electron densities and ionization energies due to molecular bonding do not significantly influence the electron-loss cross sections. Further confirmation of this hypothesis was provided by comparisons of the individual cross sections as a function of Δq, which showed only a slight dependence on the molecular nature of the target at the higher values of Δq.

ACKNOWLEDGMENTS

We are indebted to Don May, John Shumbera, and the rest of the operations staff of the Cyclotron Institute for their invaluable assistance. We thank K. E. Zaharakis for his help with some of the measurements. This work was supported by the Robert A. Welch Foundation and the DOE Office of Fusion Energy Sciences.

[1] D. Mueller, L. Grisham, I. Kaganovich, R. L. Watson, V. Horvat, K. E. Zaharakis, and M. S. Armel, Phys. Plasmas **8**, 1753 (2001).
[2] R. E. Olson, Nucl. Instrum. Methods Phys. Res. A **464**, 93 (2001).
[3] V. P. Shevelko, I. Yu. Tolstikhina, and Th. Stöhlker, Nucl. Instrum. Methods Phys. Res. B **184**, 295 (2001).
[4] R. E. Olson, R. L. Watson, V. Horvat, and K. E. Zaharakis, J. Phys. B **35**, 1893 (2002).
[5] E. C. Montenegro, W. E. Meyerhof, and J. H. McGuire, Adv. At., Mol., Opt. Phys. **34**, 249 (1994).
[6] E. C. Montenegro, W. E. Meyerhof, J. H. McGuire, and C. L. Cocke, in *The Physics of Electronic and Atomic Collisions*, edited by L. J. Dubé, J. B. A. Mitchell, J. W. McConkey, and C. E. Brion, AIP Conf. Proc. No. 360 (AIP, Woodbury, NY, 1995), p. 515.
[7] W. S. Melo, M. M. Sant'Anna, A. C. F. Santos, G. M. Sigaud, and E. C. Montenegro, Phys. Rev. A **60**, 1124 (1999).
[8] A. Mueller, B. Schuch, W. Groh, E. Salzborn, H. F. Beyer, P. H. Molker, and R. E. Olson, Phys. Rev. A **33**, 3010 (1986).
[9] R. E. Olson, in *Atomic, Molecular, and Optical Physics Handbook*, edited by G. W. F. Drake (AIP, Woodbury, NY, 1996), Chap. 56.
[10] K. Knudsen, C. D. Moak, C. M. Jones, P. D. Miller, R. O. Sayer, G. D. Alton, and L. B. Bridwell, Phys. Rev. A **19**, 1029 (1979).
[11] G. D. Alton, L. B. Bridwell, M. Lucas, C. D. Moak, P. D. Miller, C. M. Jones, Q. C. Kessel, A. A. Antar, and M. D. Brown, Phys. Rev. A **23**, 1073 (1981).
[12] L. C. Northcliffe and R. F. Schilling, Nucl. Data, Sect. A **7**, 233 (1970).
[13] A. B. Wittkower and H. D. Betz, J. Phys. B **4**, 1173 (1971).
[14] G. Bissinger, J. M. Joyce, G. Lapicki, R. Laubert, and S. L. Varghese, Phys. Rev. Lett. **49**, 318 (1982).
[15] J. M. Sanders, S. L. Varghese, and C. H. Fleming, in *Application of Accelerators in Research and Industry*, edited by J. L. Duggan and I. L. Morgan, AIP Conf. Proc. No. **576** (AIP, Melville, NY, 2001), p. 209.
[16] L. H. Toburen, M. Y. Nakai, and R. A. Langley, Phys. Rev. **171**, 114 (1968).
[17] H. Tawara and A. Russek, Rev. Mod. Phys. **45**, 178 (1973).
[18] W. G. Graham, K. H. Berkner, R. V. Pyle, A. S. Schlachter, J. W. Stearns, and J. A. Tanis, Phys. Rev. A **30**, 722 (1984).
[19] N. Bohr, K. Dan. Vidensk. Selsk. Mat. Fys. Medd. **18**, No. 8 (1948).
[20] R. E. Olson, K. H. Berkner, W. G. Graham, R. V. Pyle, A. S. Schlachter, and J. W. Stearns, Phys. Rev. Lett. **41**, 163 (1978).
[21] T. Tonuma, H. Shibata, S. H. Be, H. Kumagai, M. Kase, T. Kambera, I. Kohono, A. Ohsaki, and H. Tawara, Phys. Rev. A **33**, 3047 (1986).
[22] I. Ben-Itzhak, T. J. Gray, J. C. Legg, and J. H. McGuire, Phys. Rev. A **37**, 3685 (1988).
[23] O. Heber, G. Sampoll, B. B. Bandong, R. J. Maurer, E. Moler, R. L. Watson, I. Ben-Itzhak, J. L. Shinpaugh, J. M. Sanders, L. Hefner, and P. Richard, Phys. Rev. A **39**, 4898 (1989).
[24] O. Heber, R. L. Watson, G. Sampoll, and B. B. Bandong, Phys. Rev. A **42**, 6466 (1990).
[25] H. Knudsen, H. K. Haugen, and P. Hvelplund, Phys. Rev. A **24**, 2287 (1981).